


# Cooperative behaviors of coupled nonidentical oscillators with the same equilibrium points

Wen Sun(孙文), Biwen Li(李必文), Wanli Guo(郭万里), Zhigang Zheng(郑志刚), and Shihua Chen(陈士华)
**Citation:**Chin. Phys. B, 2021, 30 (**10**): 100504. DOI: 10.1088/1674-1056/abf101
Journal homepage: http://cpb.iphy.ac.cn; http://iopscience.iop.org/cpb

**What follows is a list of articles you may be interested in**

---

## Dynamic modeling and aperiodically intermittent strategy for adaptive finite-time synchronization control of the multi-weighted complex transportation networks with multiple delays

Ning Li(李宁), Haiyi Sun(孙海义), Xin Jing(靖新), and Zhongtang Chen(陈仲堂)
Chin. Phys. B, 2021, 30 (**9**): 090507. DOI: 10.1088/1674-1056/abea92

## Applying a global pulse disturbance to eliminate spiral waves in models of cardiac muscle

Jian Gao(高见), Changgui Gu(顾长贵), and Huijie Yang(杨会杰)
Chin. Phys. B, 2021, 30 (**7**): 070501. DOI: 10.1088/1674-1056/abf553

## Collective stochastic resonance behaviors of two coupled harmonic oscillators driven by dichotomous fluctuating frequency

Lei Jiang(姜磊), Li Lai(赖莉), Tao Yu(蔚涛), Maokang Luo(罗懋康)
Chin. Phys. B, 2021, 30 (**6**): 060502. DOI: 10.1088/1674-1056/abd9b0

## Control of chaos in Frenkel-Kontorova model using reinforcement learning

You-Ming Lei(雷佑铭) and Yan-Yan Han(韩彦彦)
Chin. Phys. B, 2021, 30 (**5**): 050503. DOI: 10.1088/1674-1056/abd74f

## Energy feedback and synchronous dynamics of Hindmarsh-Rose neuron model with memristor

K Usha, P A Subha
Chin. Phys. B, 2019, 28 (**2**): 020502. DOI: 10.1088/1674-1056/28/2/020502

---

# Cooperative behaviors of coupled nonidentical oscillators with the same equilibrium points*

Wen Sun(孙文)[1,†], Biwen Li(李必文)[1], Wanli Guo(郭万里)[2], Zhigang Zheng(郑志刚)[3], and Shihua Chen(陈士华)[4]

[1] School of Mathematics and Statistics, Hubei Normal University, Huangshi 435002, China
[2] School of Mathematics and Physics, China University of Geosciences, Wuhan 430074, China
[3] College of Information Science and Engineering, Huaqiao University, Xiamen 361021, China
[4] College of Mathematics and Statistics, Wuhan University, Wuhan 430072, China

(Received 20 January 2021; revised manuscript received 26 February 2021; accepted manuscript online 23 March 2021)

The cooperative behaviors resulted from the interaction of coupled identical oscillators have been investigated intensively. However, the coupled oscillators in practice are nonidentical, and there exist mismatched parameters. It has been proved that under certain conditions, complete synchronization can take place in coupled nonidentical oscillators with the same equilibrium points, yet other cooperative behaviors are not addressed. In this paper, we further consider two coupled nonidentical oscillators with the same equilibrium points, where one oscillator is convergent while the other is chaotic, and explore their cooperative behaviors. We find that the coupling mode and the coupling strength can bring the coupled oscillators to different cooperation behaviors in unidirectional or undirected couplings. In the case of directed coupling, death islands appear in two-parameter spaces. The mechanism inducing these transitions is presented.

**Keywords:** amplitude death, bounded chaotic synchronization, mismatched parameter

**PACS:** 05.45.Xt, 05.45.Gg **DOI:** 10.1088/1674-1056/abf101

## 1. Introduction

Due to potential applications in biological and social systems, coupled identical oscillators have received much attention recently.[1,2] The vibration behavior is a common phenomenon appearing in them and is useful for fault diagnosis.[3,4] In addition to this, lots of cooperative phenomena such as complete synchronization (CS), amplitude death (AD), and oscillation death (OD) happen on account of their interactions with other oscillators.[5–8] CS means the complete coincidence of the states of all oscillators no matter what the states will be, which appears only if the interacting oscillators are identical.[9–11] If the oscillators cannot achieve CS by themselves, various approaches such as linear feedback control,[12–15] adaptive control,[16–19] pinning control,[20–23] time-triggered impulsive control,[24–26] event-triggered impulsive control,[27,28] and sampled control[29] have been put forward to guide all the oscillators to reach the desired goal. AD refers to a coupling-induced suppression of oscillating by stabilizing an existing homogeneous steady state.[30] It is a special form of complete synchronization, that is, not only the states of all oscillators are coincident, but also the amplitudes of all oscillators are zero. Yamaguchi and Shimizu considered Kuramoto oscillators and found that sufficiently strong coupling and sufficient wide distribution of natural frequencies are needed for amplitude death to be stable.[31] Since amplitude death corresponds to the cessation of rhythmicity in a system and may be relevant to certain pathology of biological oscillators, it has drawn greater attention. Mirollo and Strogatz analyzed an array of coupled limit-cycle oscillators with mean-field coupling and randomly distributed natural frequencies, found the conditions that the system underwent amplitude death, and determined the region for which amplitude death was stable.[32] Atay studied amplitude death phenomenon theoretically in distributed time-delay.[33] Prasad found that amplitude death can occur in identical as well nonidentical coupled chaotic systems by delayed coupling.[34,35] Liu and Yang discovered the partial amplitude death in coupled chaotic oscillators when the interaction was strong enough.[36,37] Kruths analyzed the mechanisms of amplitude versus oscillation death in oscillation quenching.[38] Different from AD, OD is characterized by a newly born inhomogeneous steady state. It has been reported that CS (including AD) is impossible except that the nonidentical oscillators have the same equilibrium points.[39]

A common feature in the above works is that all the oscillators are assumed to have similar dynamics, either chaotic or periodic. However, many nonidentical oscillators in practice have entirely different dynamics. A well-known example is the Lorenz oscillator which has chaotic or convergent or periodic dynamic behavior when some parameter goes through

*Project supported by the National Natural Science Foundation of China (Grant No. 11875135) and Fundamental Research Funds for National University, China University of Geosciences (Wuhan) (Grant No. CUGGC05).

†Corresponding author. E-mail: sunwen_2201@163.com

© 2021 Chinese Physical Society and IOP Publishing Ltd 

a change. It is challenging to explore what kinds of cooperative behaviors can emerge in coupled nonidentical oscillators with the same equilibrium points, whose dynamics are totally different. We find that a new regime called bounded chaotic synchronization (BCS) can also happen besides AD. In this regime, the errors satisfy $\lim_{t\to\infty}\|Y(t)-X(t)\| \le \varepsilon$ for some $\varepsilon > 0$, and two oscillators are chaotic, especially whose maximum Lyapunov exponent is positive. More specifically, in the unidirectionally coupled oscillators, AD and BCS are determined by coupling strength and coupling directivity. In the undirected coupled oscillators, the coupling strength can bring the oscillators to different cooperative behaviors. As the coupling increases, the transition from a nonsynchronous state to a non-chaotic synchronization-AD happens. When the coupling is larger than a threshold value, two coupled oscillators are revived again from AD, and BCS occurs. In the directed and weighted coupled oscillators, death islands are established in two-parameter spaces. We show that these transitions are related to the changes in the spectrum of Lyapunov exponents (LE).

The rest of the paper is organized as follows. In Section 2, we present our considered model. In Section 3, we demonstrate amplitude death and bounded chaotic synchronization of two coupled nonidentical oscillators with different coupling modes and coupling strength. Finally, a brief summary is made in Section 4.

## 2. Theoretical analysis and experimental results

The isolated Lorenz oscillator is described as

$$\begin{cases} \dot{x} = a(y-x), \\ \dot{y} = x(28-z)-y, \\ \dot{z} = xy - \frac{8}{3}z, \end{cases} \tag{1}$$

where $a$ is a variable parameter. The three fixed points are $O=(0,0,0)$, $P^+=(\sqrt{b(r-1)},\sqrt{b(r-1)},r-1)$, and $P^-=(-\sqrt{b(r-1)},-\sqrt{b(r-1)},r-1)$, where $O$ is unstable regardless of $a$, and the eigenvalues of the other two fixed points $P^+$ and $P^-$ are the same and is dependent on $a$. The two largest Lyapunov exponents are depicted in Fig. 1 as parameter $a$ varies. It is clear that the two largest Lyapunov exponents are negative when $a$ is smaller than $a_0 = 4.0$, which implies that $P^+$ and $P^-$ are stable. When $a$ is larger than $a_0 = 4.0$, Lorenz system is chaotic since it has one positive Lyapunov exponent, one negative Lyapunov exponent and one zero Lyapunov exponent (omitted here).

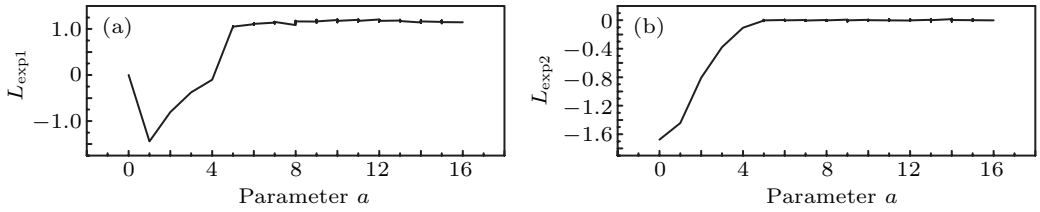



**Fig. 1.** The two largest Lyapunov exponents versus parameter $a$ for a single Lorenz system.

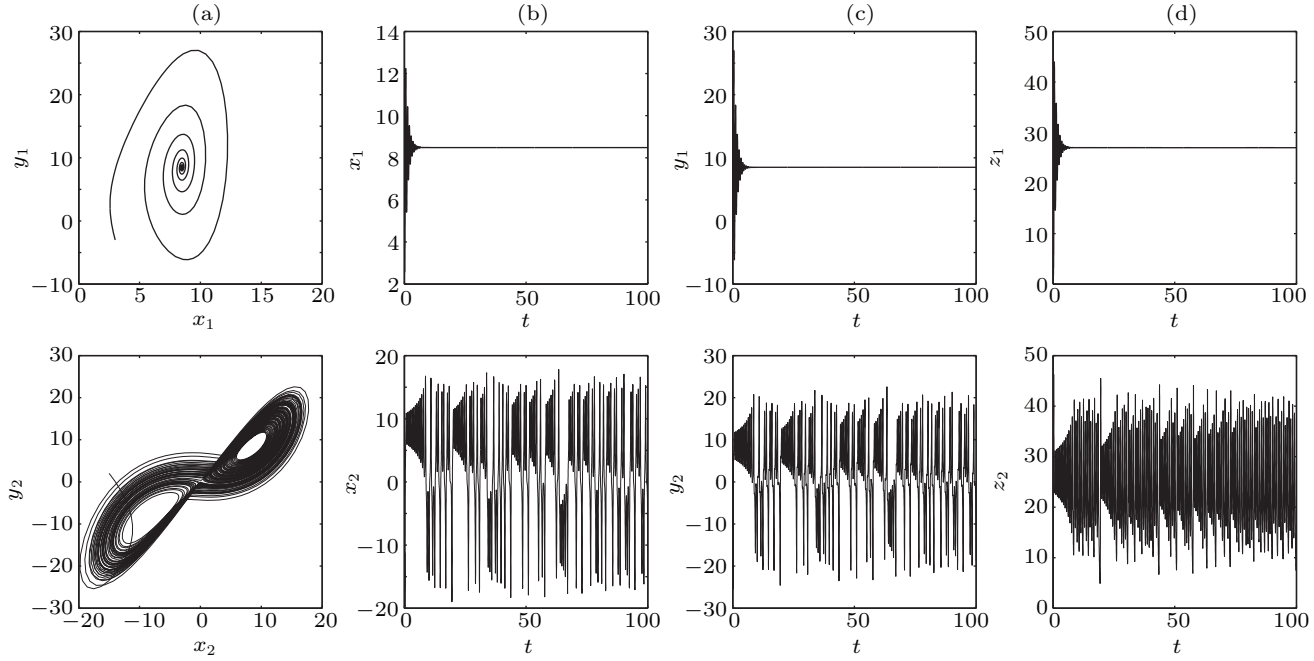



**Fig. 2.** The dynamics of two uncoupled oscillators with initial value $(3,-3,1,15,2,3)$. (a) The phase portraits in the $x$–$y$ plane. (b) The time sequence of $x$. (c) The time sequence of $y$. (d) The time sequence of $z$. The top are for the oscillator 1 and the bottom for the oscillator 2.

Two coupled Lorenz oscillators can be described by

$$\begin{cases} \dot{x}_1 = a_1(y_1 - x_1) + d_1(x_2 - x_1), \\ \dot{y}_1 = x_1(r - z_1) - y_1, \\ \dot{z}_1 = x_1 y_1 - b z_1, \\ \dot{x}_2 = a_2(y_2 - x_2) + d_2(x_1 - x_2), \\ \dot{y}_2 = x_2(r - z_2) - y_2, \\ \dot{z}_2 = x_2 y_2 - b z_2, \end{cases} \tag{2}$$

where $a_1 = 1$ and $a_2 = 12$ are mismatched parameters. $d_{1,2}$ are the coupling strengths. In the absence of coupling, oscillator 1 is unchaotic, and its trajectories converge to its fixed points $P^+$ or $P^-$ depending on the initial condition; while oscillator 2 displays chaotic motion for the same initial value $(3,-3,1,15,2,3)$, which can be seen from Fig. 2.

For convenience, Eq. (2) can be written as

$$\begin{cases} \dot{X}(t) = f_{a_1}(t, X(t)) + d_1 \Gamma (Y(t) - X(t)), \\ \dot{Y}(t) = f_{a_2}(t, Y(t)) + d_2 \Gamma (X(t) - Y(t)), \end{cases} \tag{3}$$

where $X = (x_1, x_2, x_3)^{\mathrm{T}}$, $Y = (y_1, y_2, y_3)^{\mathrm{T}} \in R^3$. $f_{a_1}$, $f_{a_2}$ : $R^n \times [0,\infty] \longrightarrow R^n$ are continuous vector functions. $\Gamma = \mathrm{diag}\{1,0,0\}$ is the inner coupling matrix, which represents the inner coupled configuration between two oscillators. We assume that two uncoupled oscillators $\dot{X}(t) = f_{a_1}(t, X(t))$ and $\dot{Y}(t) = f_{a_2}(t, Y(t))$ have the same equilibrium points, i.e., $f_{a_1}(t, X^*) = f_{a_2}(t, X^*) = 0$. Furthermore, $f_{a_1}(t, X), f_{a_2}(t, Y) \in C([0,\infty) \times R^n, R^n)$ satisfy

$$\begin{aligned} & (X_1 - X_2)^{\mathrm{T}} [f_{a_1}(t, X_1) - f_{a_1}(t, X_2) - k_1 \Gamma (X_1 - X_2)] \\ \le & -\varepsilon_1 (X_1 - X_2)^{\mathrm{T}} (X_1 - X_2), \\ & (Y_1 - Y_2)^{\mathrm{T}} [f_{a_2}(t, Y_1) - f_{a_2}(t, Y_2) - k_2 \Gamma (Y_1 - Y_2)] \\ \le & -\varepsilon_2 (Y_1 - Y_2)^{\mathrm{T}} (Y_1 - Y_2), \end{aligned}$$

for $k_1 > 0$, $k_2 > 0$, $\varepsilon_1 > 0$, $\varepsilon_2 > 0$, $X_1, X_2, Y_1, Y_2 \in R^n$ and $t > 0$.

This assumption is moderate, and many chaotic systems such as Chua's oscillators, Rössler systems, Lorenz systems, Chen systems, and Lü systems satisfy this assumption.

### 2.1. Unidirectional couplings

(I) While $d_1 \neq 0$, $d_2 = 0$, the chaotic oscillator is the drive system, while the nonchaotic oscillator is the response system, Eq. (2) is turned into

$$\begin{cases} \dot{X}(t) = f_{a_1}(t, X(t)) + d_1 \Gamma (Y(t) - X(t)), \\ \dot{Y}(t) = f_{a_2}(t, Y(t)). \end{cases} \tag{4}$$

Let $e(t) = X(t) - Y(t)$, and choose a Lyapunov function candidate as

$$V(e(t)) = \frac{1}{2} e(t)^{\mathrm{T}} e(t).$$

The derivative of $V(e(t))$ along the trajectories of Eq. (4) is

$$\begin{aligned} \dot{V}(e(t)) &= e^{\mathrm{T}}(t)[f_{a_1}(t, X(t)) - f_{a_2}(t, Y(t)) - d_1 \Gamma e(t)] \\ &= e^{\mathrm{T}}(t)[f_{a_1}(t, X(t)) - f_{a_1}(t, Y(t)) - k_1 \Gamma e(t) \\ &\quad + (k_1 - d_1)\Gamma e(t) + f_{a_1}(t, Y(t)) - f_{a_2}(t, Y(t))] \\ &\le -\varepsilon_1 e^{\mathrm{T}}(t) e(t) + e^{\mathrm{T}}(t)[(k_1 - d_1)\Gamma e(t) \\ &\quad + f_{a_1}(t, Y(t)) - f_{a_2}(t, Y(t))] \\ &\le -\varepsilon_1 \|e(t)\|^2 + (k_1 - d_1) e^{\mathrm{T}}(t) \Gamma e(t) \\ &\quad + \|e(t)\| \|f_{a_1}(t, Y(t)) - f_{a_2}(t, Y(t))\|. \end{aligned}$$

Since the drive system $Y(t)$ is chaotic and bounded, then $f_{a_2}(t, Y(t))$, $f_{a_1}(t, Y(t))$ are nonzero and bounded. Because of the continuity of $f_{a_1}(\cdot)$, $f_{a_2}(\cdot)$, we assume $M_1 = \max\{\|f_{a_2}(t, Y(t)) - f_{a_1}(t, Y(t))\|\}$. Thus,

$$\begin{aligned} & \dot{V}(e(t)) \\ \le & -\varepsilon_1 \|e(t)\|^2 + (k_1 - d_1)\|\Gamma\| \|e(t)\|^2 + \|e(t)\| M_1 \\ \le & -\varepsilon_1 \|e(t)\|^2 + (k_1 - d_1)\|\Gamma\| \|e(t)\|^2 + \gamma_1 \|e(t)\|^2 + \frac{1}{\gamma_1} M_1^2 \\ = & -\varepsilon_1 \|e(t)\|^2 + [(k_1 - d_1)\|\Gamma\| + \gamma_1] \|e(t)\|^2 + \frac{1}{\gamma_1} M_1^2, \end{aligned}$$

where $\gamma_1 > 0$.

If $(k_1 - d_1)\|\Gamma\| + \gamma_1 \le 0$, then

$$\dot{V}(e(t)) \le -\varepsilon \|e(t)\|^2 + \frac{1}{\gamma_1} M_1^2 = -2\varepsilon V(e(t)) + \frac{1}{\gamma_1} M_1^2.$$

We get

$$V(e(t)) \le V(e(0))\, \mathrm{e}^{-2\varepsilon t} + \frac{M_1^2}{2\varepsilon\gamma_1},$$

and $\|e(t)\| \le \sqrt{M_1^2/(\varepsilon\gamma_1)}$. Therefore, bounded chaotic synchronization takes place.

Figure 3 illustrates the two largest Lyapunov exponents versus the coupling strength $d_1$, in which the first-largest Lyapunov exponent is positive while the second-largest Lyapunov exponent is zero with $d_1$ increasing. Figure 4 shows the phase portraits in the $x$–$y$ plane for two unidirectional coupled oscillators with the coupling strength $d_1 = 20$ in (a) and the time sequences of $x$, $y$, $z$ in (b), (c) and (d). It is clear that the unchaotic oscillator 1 can synchronize to the chaotic trajectories of oscillator 2. Bounded chaotic synchronization (BCS) occurs.

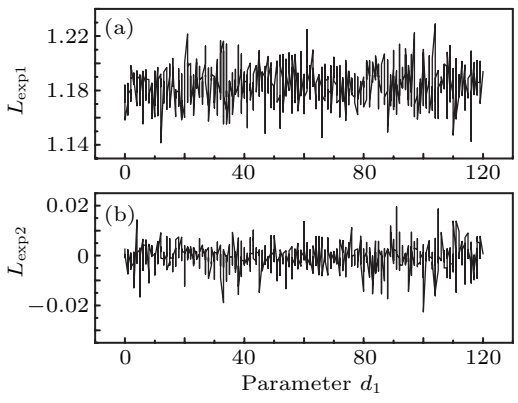



**Fig. 3.** The two largest Lyapunov exponents versus the coupling strength $d_1$ ($d_2 = 0$) for two unidirectional coupled oscillators.

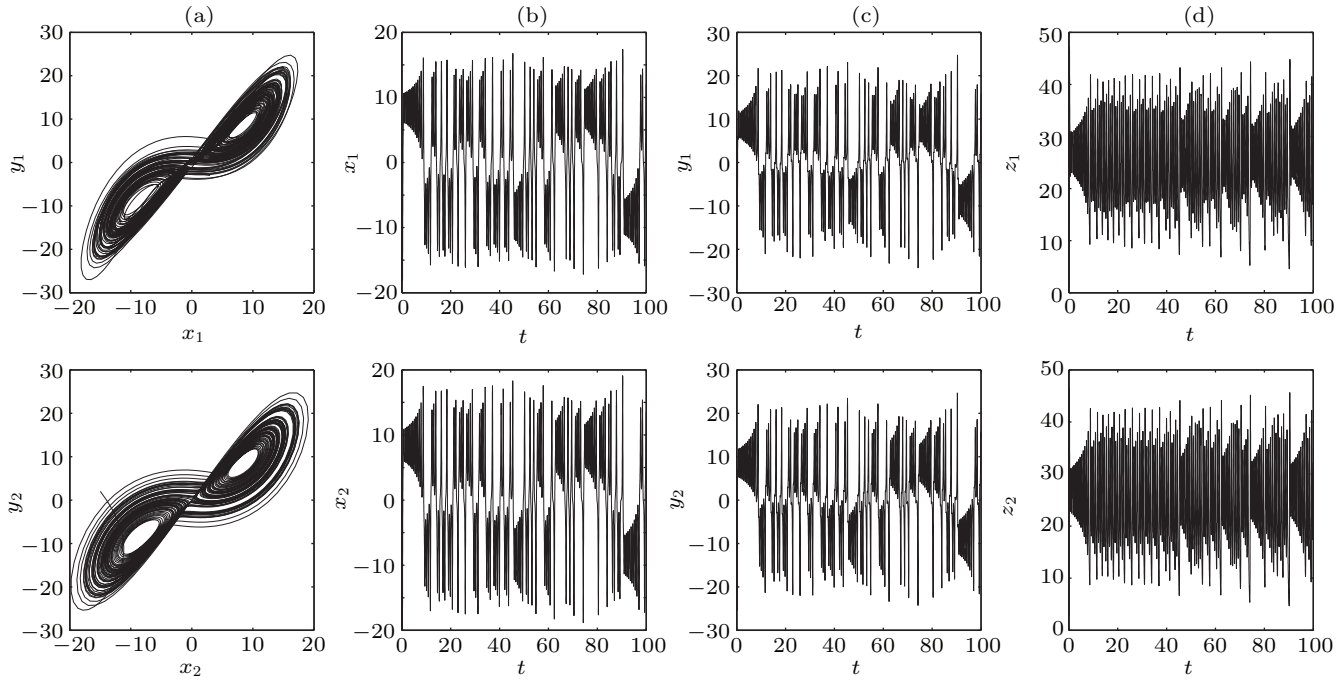



**Fig. 4.** The dynamics of two unidirectional coupled oscillators with the coupling strength $d_1 = 20$ ($d_2 = 0$) and initial value $(3,-3,1,15,2,3)$. (a) The phase portraits in the $x$–$y$ plane. (b) The time sequence of $x$. (c) The time sequence of $y$. (d) The time sequence of $z$.

(II) When $d_1 = 0$, $d_2 \neq 0$, the chaotic oscillator is the response system, while the nonchaotic oscillator is the drive system, Eq. (2) is changed into

$$\begin{cases} \dot{X}(t) = f_{a_1}(t, X(t)), \\ \dot{Y}(t) = f_{a_2}(t, Y(t)) + d_2 \Gamma (X(t) - Y(t)). \end{cases} \tag{5}$$

The derivative of $V(e(t))$ along the trajectories of Eq. (5) is

$$\begin{aligned} \dot{V}(e(t)) &= e^{\mathrm{T}}(t)[f_{a_1}(t, X(t)) - f_{a_2}(t, Y(t)) - d_2 \Gamma e(t)] \\ &= e^{\mathrm{T}}(t)[f_{a_2}(t, X(t)) - f_{a_2}(t, Y(t)) - k_2 \Gamma e(t) \\ &\quad + (k_2 - d_2)\Gamma e(t) + f_{a_1}(t, X(t)) - f_{a_2}(t, X(t))] \\ &\leq -\varepsilon_2 e^{\mathrm{T}}(t) e(t) + e^{\mathrm{T}}(t)[(k_2 - d_2)\Gamma e(t) \\ &\quad + f_{a_1}(t, X(t)) - f_{a_2}(t, X(t))] \\ &\leq -\varepsilon_2 \|e(t)\|^2 + (k_2 - d_2) e^{\mathrm{T}}(t) \Gamma e(t) \\ &\quad + \|e(t)\| \|f_{a_1}(t, X(t)) - f_{a_2}(t, X(t))\|. \end{aligned}$$

Since the drive system $X(t)$ converges to one of its equilibrium points, then $f_{a_2}(t, X(t)) = f_{a_1}(t, X(t)) = 0$. Thus,

$$\dot{V}(e(t)) \leq -\varepsilon_2 \|e(t)\|^2 + (k_2 - d_2) \|\Gamma\| \|e(t)\|^2.$$

If $k_2 - d_2 \leq 0$, then $\dot{V}(e(t)) \leq -\varepsilon_2 \|e(t)\|^2$. We get $V(e(t)) \leq V(e(0))\, \mathrm{e}^{-2\varepsilon_2 t}$. Thus, $e(t) \to 0$ and amplitude death occurs.

Figure 5 illustrates the two largest Lyapunov exponents versus the coupling strength $d_2$, in which the first-largest and the second-largest Lyapunov exponents are negative as the coupling strength $d_2$ increases. Under the drive of oscillator 1, the chaotic oscillator 2 can evolve into one of two fixed points of oscillator 1 depending on the initial condition and does not run away since that is also its own equilibrium point. Namely, amplitude death appears. Figure 6 shows the phase portraits in the $x$–$y$ plane for two unidirectional coupled oscillators with the coupling strength $d_2 = 30$ in (a) and the time sequences of the variable $x$, $y$, $z$ in (b), (c) and (d).

In the unidirectional coupled non-identical oscillators, the response system can synchronize to the drive system even with mismatched parameters. Different synchronization pattern of BS is mainly regulated by the strength and the directivity of the coupling $d_1$ ($d_2$).

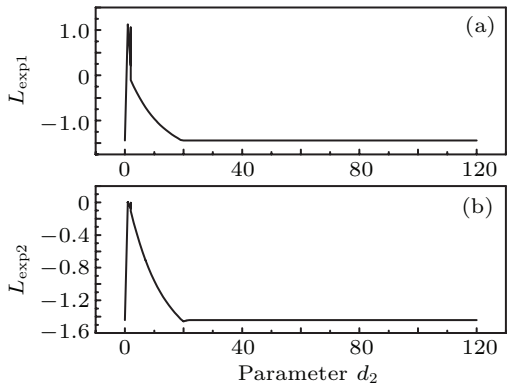



**Fig. 5.** The two largest Lyapunov exponents versus the coupling strength $d_2$ ($d_1 = 0$) for two unidirectional coupled oscillators.

When the couplings are undirected or directed, theoretical analysis similar to the above is very difficult due to the heterogeneity of nonidentical oscillators. However, we get some interesting numerical results.

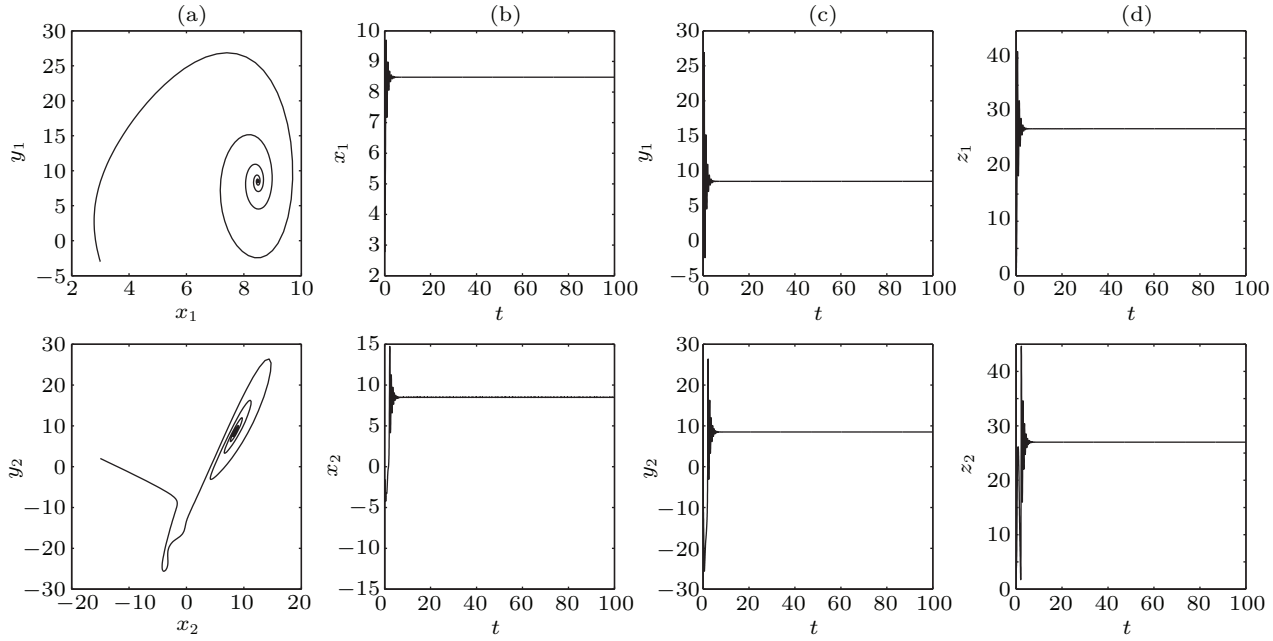



**Fig. 6.** The dynamics of two unidirectional coupled oscillators with the coupling strength $d_2 = 20$ ($d_1 = 0$) and initial value $(3, -3, 1, 15, 2, 3)$. (a) The phase portraits in the $x$–$y$ plane. (b) The time sequence of $x$. (c) The time sequence of $y$. (d) The time sequence of $z$.

## 2.2. Undirected couplings

When the coupling is undirected, the dynamics of the coupled oscillators are more complex and controlled by the coupling strength $d$. As the coupling strength increases, some intriguing new phenomena can occur. The two largest Lyapunov exponents versus the coupling strength $d$ are plotted in Fig. 7.

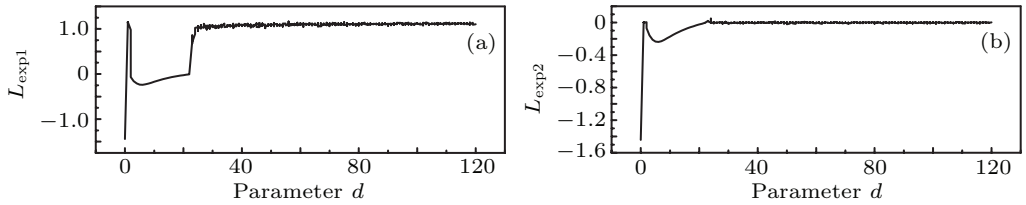



**Fig. 7.** The two largest Lyapunov exponents versus the coupling strength $d$ for two undirected coupled Lorenz systems.

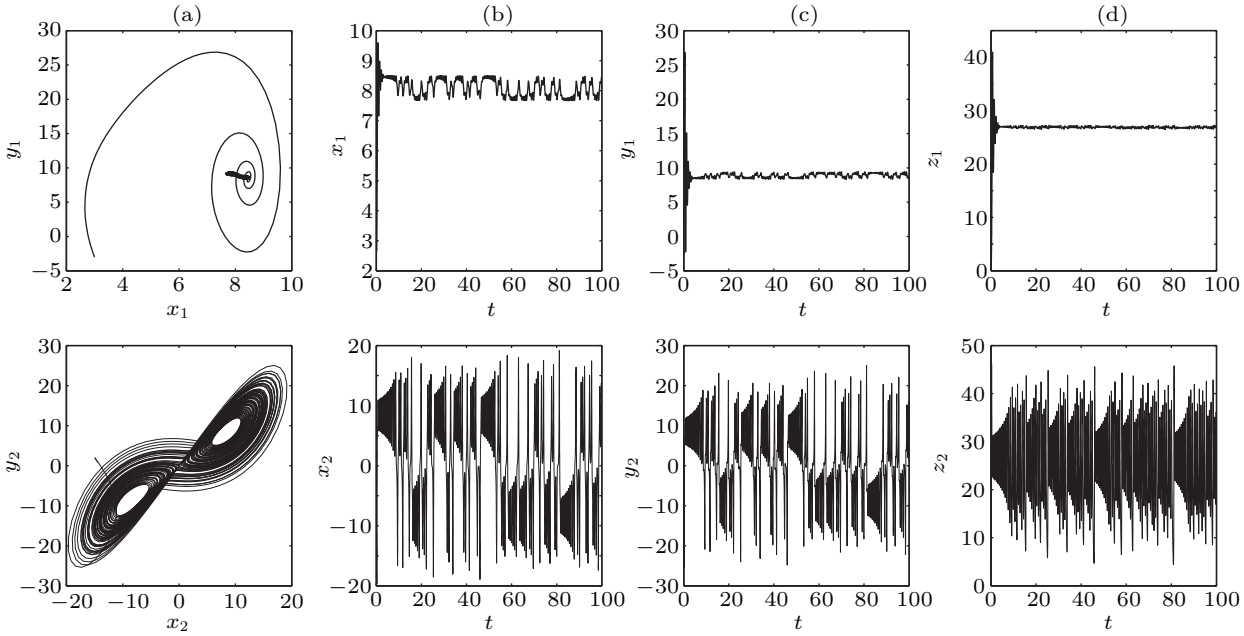



**Fig. 8.** The dynamics of two undirected coupled oscillators with the coupling strength $d = 0.1$ and initial value $(3, -3, 1, 15, 2, 3)$. (a) The phase portraits in the $x$–$y$ plane. (b) The time sequence of $x$. (c) The time sequence of $y$. (d) The time sequence of $z$.

From Fig. 7, we can see that the two largest Lyapunov exponents are negative when $d_1^0 < d < d_2^0$, creating a death interval $(d_1^0, d_2^0)$, and that the two largest Lyapunov exponents are positive when $d \geq d_2^0$, generating chaotic synchronization interval $(d_2^0, +\infty)$, where $d_1^0 \approx 1.2$, $d_2^0 \approx 22.0$. The coupling strength $d$ can bring the oscillators to the AD state when $d_1^0 < d < d_2^0$ and again can revive the systems to oscillatory states when $d \geq d_2^0$.

To get more information about the dynamical behaviors implicit in Fig. 7, we depict the phase portraits and the time sequences of $x$, $y$, and $z$. As the coupling between the oscillators is turned on, especially the coupling strength $d$ is very small, the interaction between them is not enough to change their dynamics much. Oscillator 1 oscillates near its equilibrium point, while oscillator 2 oscillates near its chaotic trajectories. Figure 8 shows the phase portraits in the $x$–$y$ plane for two undirected coupled oscillators with $d = 0.1$ in (a) and the time sequences of $x$, $y$, $z$ in (b), (c) and (d).

As the coupling strength $d$ increases to the interval $(d_1^0, d_2^0)$, oscillator 1 pulls the chaotic trajectories of oscillator 2 to its equilibrium point. Figure 9 shows the phase portraits in the $x$–$y$ plane for two undirected coupled oscillators with $d = 20$ in (a) and the time sequences of $x$, $y$, $z$ in (b), (c) and (d). Old fixed points are stabilized again by the coupling and become the attractors of the whole system.

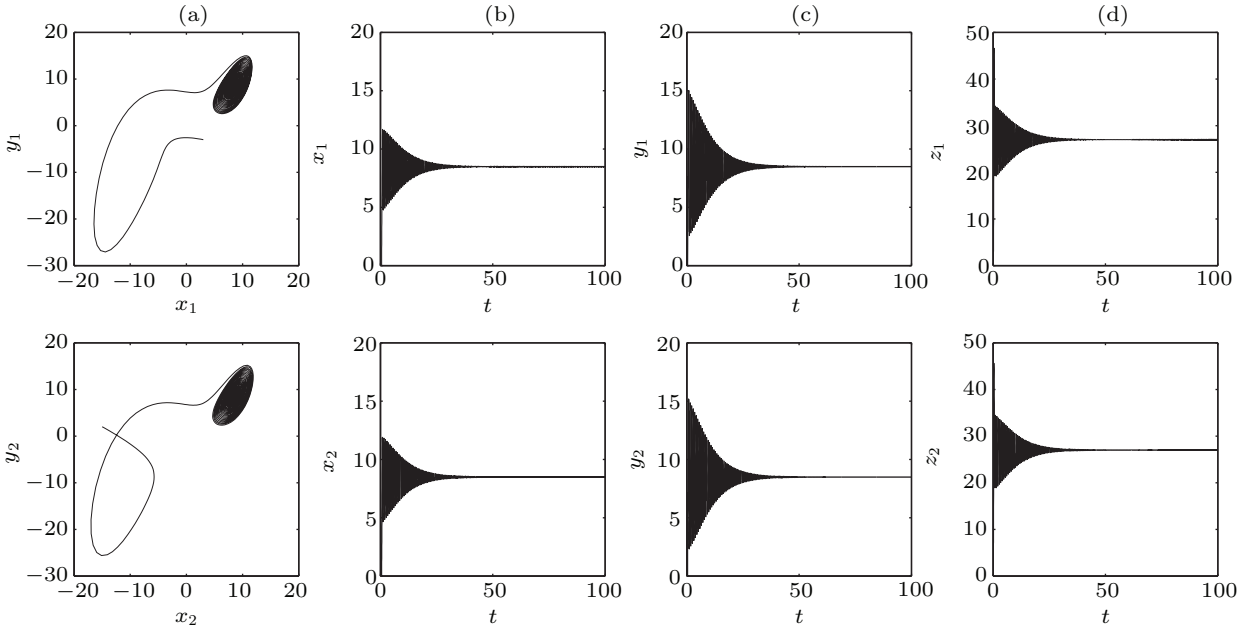



**Fig. 9.** The dynamics of two undirected coupled oscillators with the coupling strength $d = 20$ and initial value $(3, -3, 1, 15, 2, 3)$. (a) The phase portraits in the $x$–$y$ plane. (b) The time sequence of $x$. (c) The time sequence of $y$. (d) The time sequence of $z$.

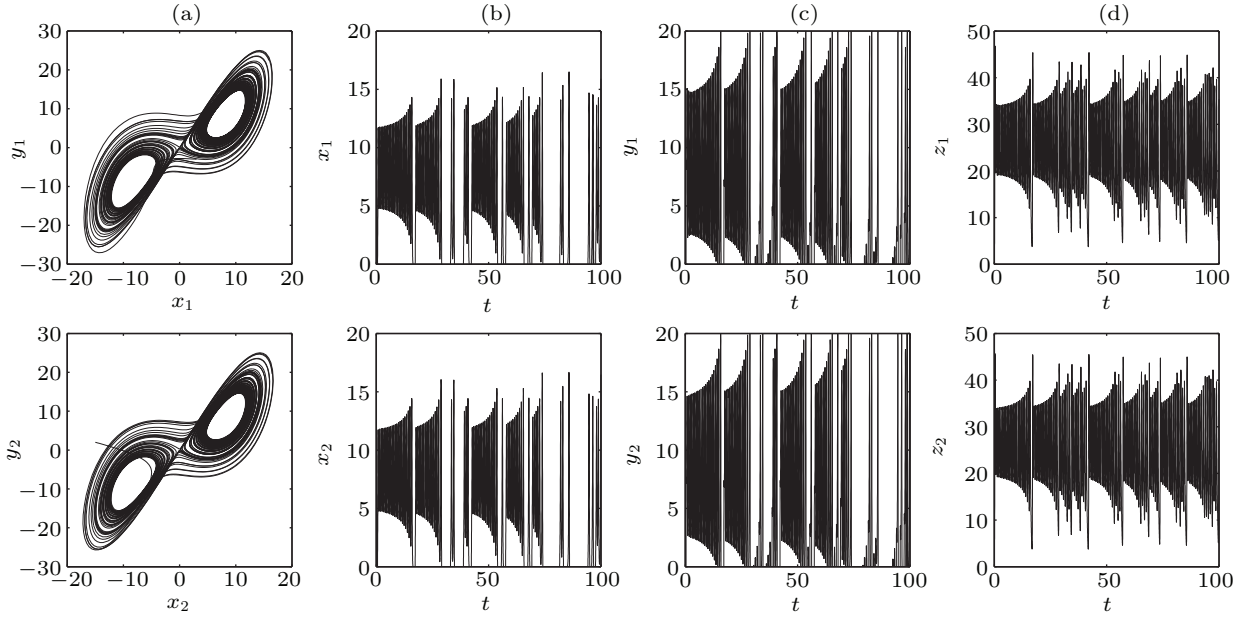



**Fig. 10.** The dynamics of two undirected coupled oscillators with the coupling strength $d = 42$ and initial value $(3, -3, 1, 15, 2, 3)$. (a) The phase portraits in the $x$–$y$ plane. (b) The time sequence of $x$. (c) The time sequence of $y$. (d) The time sequence of $z$.

When the coupling strength $d$ goes beyond a critical coupling strength $d_2^0$, oscillator 1 can be pulled to the chaotic trajectories of oscillator 2. Figure 10 shows the phase portraits in the $x$–$y$ plane for two undirected coupled oscillators with $d = 42$ in (a) and the time sequences of $x$, $y$, $z$ in (b), (c) and (d). Interestingly enough, the AD states of oscillator 1 are revived again by the coupling and become chaotic attractors.

### 2.3. Directed couplings

When the coupling is directed and weighted, the dynamics of the coupled oscillators are regulated by two coupling strengths $d_1$ and $d_2$. The two largest Lyapunov exponents versus the coupling strength $d_1$ and $d_2$ are plotted in Fig. 11, where the two largest Lyapunov exponents are negative in the blue area and positive in the gray area. We find that different cooperative behaviors of two coupled oscillators with mismatched parameters emerge according to the variation of $d_1$ and $d_2$. In the blue lower triangular overlapping region in Figs. 11(a) and 11(b), the non-chaotic synchronization, i.e., amplitude death happens. In the other regions, the bounded chaotic synchronization takes place, resulting in the oscillators oscillating.

When we put $d_1 = 20$ and $d_2 = 4$ in the bounded chaotic synchronization region (the gray areas in Fig. 11(a) and the blue areas in Fig. 11(b)), where the first-largest Lyapunov exponent is positive while the second-largest Lyapunov exponent is negative, bounded chaotic synchronization occurs. Figure 12 shows the phase portraits in the $x$–$y$ plane for two directed and weighted coupled oscillators in (a) and the time sequences of $x$, $y$, $z$ in (b), (c) and (d), which are in agreement with Fig. 11.

When we put $d_1 = 4$ and $d_2 = 16$ in the amplitude death region (the blue areas in Figs. 11(a) and 11(b)) where the two largest Lyapunov exponents are negative, amplitude death takes place. Figure 13 shows the phase portraits in the $x$–$y$ plane for two directed and weighted coupled oscillators in (a) and the time sequences of $x$, $y$, $z$ in (b), (c) and (d).

The above analysis concludes that the coupling strength $d_1$ is intended for oscillating, while the coupling strength $d_2$ is valid for converging. Thus, there is a trade-off between making oscillators oscillate and making them convergent. The competition between the coupling strength $d_1$ and $d_2$ is the critical factor that induced these transitions between amplitude death and bounded chaotic synchronization.

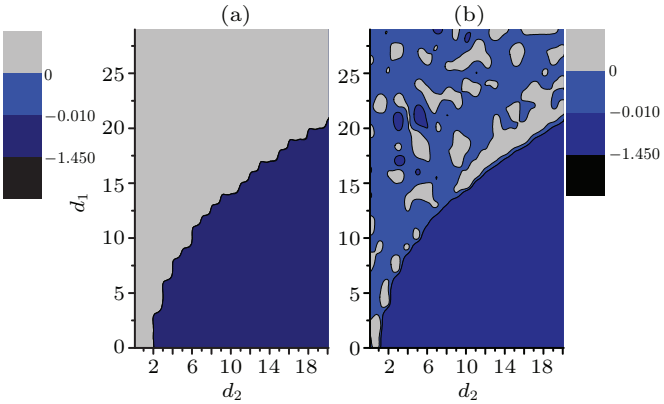



**Fig. 11.** The two largest Lyapunov exponents versus the variation of $d_1, d_2$ for two directed and weighted coupled Lorenz systems. (a) The first-largest Lyapunov exponent. (b) The second-largest Lyapunov exponent.

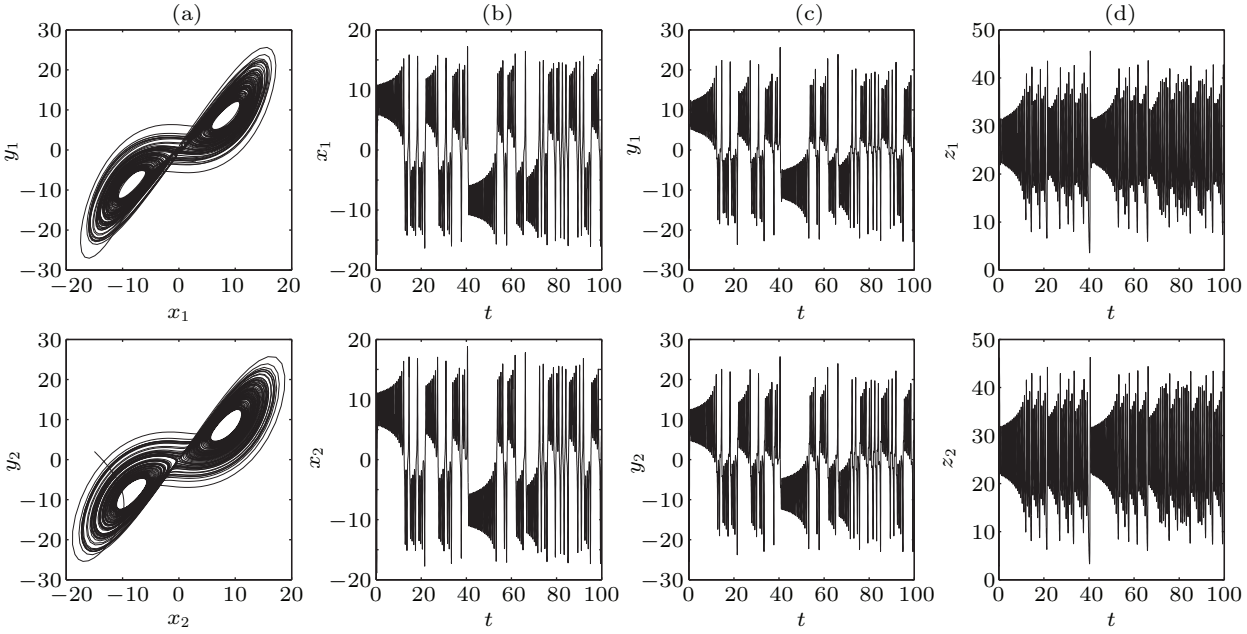



**Fig. 12.** The dynamics of two directed and weighted coupled oscillators with $d_1 = 20$, $d_2 = 4$ and initial value $(3, -3, 1, 15, 2, 3)$. (a) The phase portraits in the $x$–$y$ plane. (b) The time sequence of $x$. (c) The time sequence of $y$. (d) The time sequence of $z$.

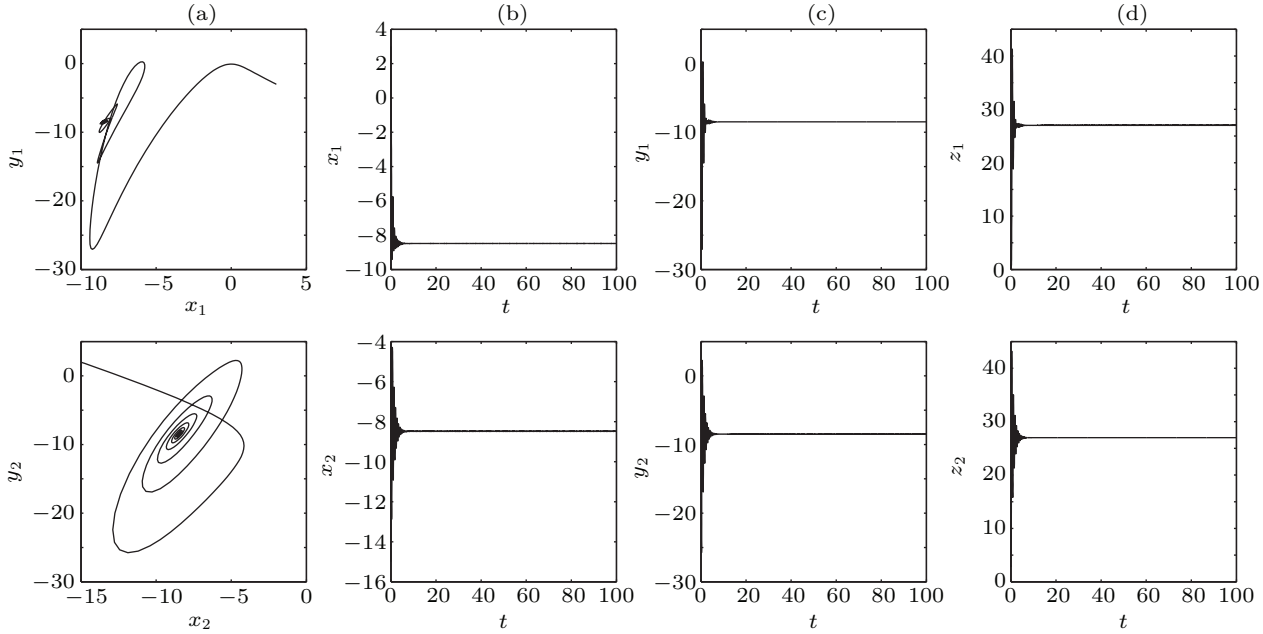



**Fig. 13.** The dynamics of two directed and weighted coupled oscillators with $d_1 = 4$, $d_2 = 16$ and initial value $(3, -3, 1, 15, 2, 3)$. (a) The phase portraits in the $x$–$y$ plane. (b) The time sequence of $x$. (c) The time sequence of $y$. (d) The time sequence of $z$.

## 3. Conclusions

We have investigated the cooperative behaviors of coupled nonidentical oscillators with the same equilibrium points, where one oscillator is convergent while the other is chaotic. We find that when the coupling is unidirectional, the responding system can easily synchronize to the driving system with the coupling strength increasing. When the coupling is undirected, it can bring the coupled oscillators to different cooperative behaviors. Specifically, the non-chaotic synchronization, including amplitude death and the existence of death intervals, occurs as the interaction is strong; while the coupling is beyond a certain threshold, bounded chaotic synchronization takes place. In the case of directed and weighted coupling, amplitude death islands appear in two-parameter spaces. Our next concern is how to use our proposed methods to revive or cease the rhythmicity of certain biological oscillators, which is helpful for the recovery of some diseases.

## References


[1] Strogatz S H 2001 *Nature* **410** 268
[2] Pan T W, Huang X, Xu C and Lü H P 2019 *Chin. Phys. B* **28** 120503
[3] Zhang G, Hu D and Zhang T 2019 *IEEE Access* **7** 58435
[4] Zhang G, Wang H and Zhang T 2020 *Results Phys.* **17** 103158
[5] Su S L, Xiao J H, Liu W Q and Wu Y 2021 *Chin. Phys. B* **30** 010505
[6] Shen J and Tang L 2018 *Chin. Phys. B* **27** 100503
[7] Tong P and Chen S H 2017 *Chin. Phys. B* **26** 050503
[8] Li C B, Thio W J, Sprott J C, Zhang R X and Lu T A 2017 *Chin. Phys. B* **26** 120501
[9] Wu Y, Shang Y, Chen M, Zhou C and Kurths J 2008 *Chaos* **18** 037111
[10] Watts D J and Strogatz S H 1998 *Nature* **393** 440
[11] Pecora L M and Carroll T L 1990 *Phys. Rev. Lett.* **64** 821
[12] Wu C W and Chua L O 1995 *IEEE Trans. Circuits Syst. I* **42** 430
[13] Lu W and Chen T 2006 *Physica D* **213** 214
[14] Chen Y, Lu J, Han F and Yu X 2011 *Syst. Contr. Lett.* **60** 517
[15] Lu J, Yu X, Chen G and Cheng D 2004 *IEEE Trans. Circuits Syst. I* **51** 787
[16] Lu J and Chen G 2005 *IEEE Trans. Automat. Contr.* **50** 841
[17] Zhou J, Lu J and Lü J 2006 *IEEE Trans. Automat. Contr.* **51** 652
[18] Mei G, Wu X, Wang Y, Hu M, Lu J and Chen G 2018 *IEEE Trans. Cyber.* **48** 754
[19] Li Y, Wu X, Lu J and Lu J 2016 *IEEE Trans. Circuits Syst. II* **63** 206
[20] Wang X and Chen G 2002 *Physica A* **310** 521
[21] Chen T, Liu X and Lu W 2007 *IEEE Trans. Circuits Syst. I* **54** 1317
[22] Yu W, Chen G and Lü J 2009 *Automatica* **45** 429
[23] Lu W, Li X and Rong Z 2010 *Automatica* **46** 116
[24] Sun W, Guan J, Lu J, Zheng Z, Yu X and Chen S 2020 *IEEE Trans. Neural Netw. Learn. Syst.* **31** 960
[25] Sun W, Chen Z and Chen S H 2012 *Chin. Phys. B* **21** 050509
[26] Sun W, Chen Z and Kang Y H 2012 *Chin. Phys. B* **21** 010504
[27] Sun W, Zheng H, Guo W, Xu Y, Cao J, Abdel-Aty M and Chen S 2020 *IEEE Trans. Cybern.*
[28] Sun W, Yuan Z, Lu Z, Hu J and Chen S 2020 *IEEE Trans. Cybern.*
[29] Sun W, Huang C, Lu J, Li X and Chen S 2016 *Chaos* **26** 023106
[30] Saxena G, Prasad A and Ramaswamy R 2012 *Phys. Rep.* **521** 205
[31] Yamaguchi Y and Shimizu H 1984 *Physica D* **11** 212
[32] Mirollo R E and Strogatz S H 1990 *J. Stat. Phys.* **60** 245
[33] Atay F M 2003 *Physica D* **183** 1
[34] Prasad A 2005 *Phys. Rev. E* **72** 056204
[35] Sharma A, Suresh K, Thamilmaran K, Prasad A and Shrimali M D 2014 *Nonlinear Dyn.* **76** 1797
[36] Liu W, Xiao J and Yang J 2005 *Phys. Rev. E* **72** 057201
[37] Yang J Z, Xiao J H and Liu W Q 2006 *Chin. Phys. B* **15** 2260
[38] Koseska A, Volkov E and Kruths J 2013 *Phys. Rep.* **531** 173
[39] Xiang J and Chen G 2007 *Automatica* **43** 1049